

NUMERICAL SIMULATION OF THE ACOUSTIC AND ELASTIC WAVEFIELDS RADIATED BY A SOURCE IN A FLUID-FILLED BOREHOLE EMBEDDED IN A LAYERED MEDIUM

by

Michel Bouchon

Earth Resources Laboratory
Department of Earth, Atmospheric, and Planetary Sciences
Massachusetts Institute of Technology
Cambridge, MA 02139

ABSTRACT

We present a method of calculation to simulate the propagation of acoustic and elastic waves generated by a borehole source embedded in a layered medium. The method is formulated as a boundary element technique where the Green's functions are calculated by the discrete wavenumber method. The restrictive assumptions are that the borehole is cylindrical and that its axis runs normal to the layer interfaces. The method is used to generate synthetic acoustic logs and to investigate the wavefield radiated into the formation. The simulations considered display the Stoneley wave reflections at the bed boundaries and show the importance of the diffraction which takes place where the borehole wall intersects the layer interfaces.

INTRODUCTION

Boundary integral equation methods have been used over the past few years to tackle a variety of problems in seismology (e.g., Sanchez-Sesma and Esquivel, 1979; Bouchon, 1985; Campillo, 1987a; Kawase, 1988; Kawase and Aki, 1990; Gaffet and Bouchon, 1991; Sanchez-Sesma and Campillo, 1991) and in seismic exploration (Campillo, 1987b; Paul and Campillo, 1988; Coutant, 1989; Bouchon and Schmitt, 1989; Bouchon *et al.*, 1989; Randall, 1991; Liu and Randall, 1991). These methods allow the complete calculation of the acoustic or elastic wavefield diffracted at irregular boundaries and thus can be used to simulate numerically the propagation of seismic waves in complex geological structures.

We apply here such a method to the case of a fluid-filled borehole embedded in a layered medium. We use an approach very close to the one developed by Kawase and Aki

(Kawase, 1988; Kawase and Aki, 1989) where the Green's functions are calculated by the discrete wavenumber method and where the singularities inherent to the boundary integral equation approach are removed by integrating the Green's functions over surface elements.

Previous work on this subject has been done using finite difference methods (Stephen *et al.*, 1985; Randall *et al.*, 1991) and the aim of this study is to present a workable semi-analytical alternative to a purely numerical approach.

DESCRIPTION OF THE METHOD

The problem configuration consists of a fluid-filled cylindrical borehole embedded in a layered elastic medium. The borehole walls are assumed to be normal to the interfaces between layers and the source considered is a point of dilatation located at the center of the borehole.

We define a cylindrical coordinate system (r, θ, z) centered at the source and oriented along the borehole axis. We characterize the source by its volume change $v_s(t)$. The displacement potential radiated in the fluid by the source may thus be expressed by (e.g., Kurkjian and Chang, 1986):

$$\phi_s(r, z, t) = \frac{-1}{4\pi R} v_s(t - R/\alpha_o) \quad (1)$$

where $R = (r^2 + z^2)^{1/2}$ and α_o is the fluid compressional wave velocity.

Denoting by $V_s(\omega)$ the frequency spectrum of the volume change, the Fourier transform of equation (1) gives:

$$\Phi_s(r, z, \omega) = \frac{-1}{4\pi R} V_s(\omega) e^{-i\omega R/\alpha_o}. \quad (2)$$

Because of the cylindrical geometry of the borehole problem, it is convenient to represent the spherical wave radiation expressed in equation (2) by an integral of cylindrical waves. This can be done by using either the vertical wavenumbers or the horizontal wavenumbers as eigenvectors for the cylindrical wave decomposition. The former representation is the one usually used to calculate the radiation for a borehole in a homogeneous formation (e.g., Tsang and Rader, 1979; Cheng and Toksöz, 1981; Schoenberg *et al.*, 1981; Cheng *et al.*, 1982; Tubman *et al.*, 1984; Schmitt and Bouchon, 1985; Schmitt, 1988). In the present case, however, where one needs to evaluate the Green's functions for the layered elastic formation, the decomposition must be performed, at least for the elastic Green's functions, in the horizontal wavenumber space. This is done using

Sommerfeld's integral:

$$\frac{e^{-i\omega R/\alpha_o}}{R} = -i \int_0^\infty \frac{k}{\nu} J_o(kr) e^{-i\nu|z|} dk \quad (3)$$

where $\nu = (\frac{\omega^2}{\alpha_o^2} - k^2)^{1/2}$, $Im(\nu) \leq 0$.

We then get:

$$\Phi_s(r, z, \omega) = \frac{iV_s(\omega)}{4\pi} \int_0^\infty \frac{k}{\nu} J_o(kr) e^{-i\nu|z|} dk. \quad (4)$$

The integral in equation (4) may be evaluated by the discrete wavenumber method (Bouchon, 1981) which yields:

$$\Phi_s(r, z, \omega) = \frac{iV_s(\omega)}{2L} \sum_{n=0}^M \frac{k_n}{\nu_n} J_o(k_n r) e^{-i\nu_n|z|} \quad (5)$$

with $k_n = \frac{2\pi}{L}n$; $\nu_n = (\frac{\omega^2}{\alpha_o^2} - k_n^2)^{1/2}$, $Im(\nu_n) \leq 0$ and where L is the radial periodicity associated with the discretization in wavenumber space, and M is an integer large enough to insure the convergence of the series.

Using equation (5) and denoting by ρ_o the fluid density, the radial displacement and radial stress due to the incident source wavefield

$$\begin{aligned} u_r^s &= \frac{d\Phi_s}{dr} \\ \sigma_{rr}^s &= -\rho_o \omega^2 \Phi_s \end{aligned} \quad (6)$$

may be calculated anywhere in the fluid and in particular at the borehole wall.

Each point of the borehole wall may be regarded as a secondary source of radiation (Huygens principle) and the wavefield diffracted into the fluid may be expressed as the integral over the borehole wall of a source density function τ times the Green's function for the fluid G_f :

$$\Phi_f(r, z, \omega) = \int \tau(z_o, \theta_o) G_f(r, \theta, z; r_o, \theta_o, z_o; \omega) r_o d\theta_o dz_o. \quad (7)$$

G_f is an isotropic spherical disturbance which may be expressed in the form of Sommerfeld's integral (3):

$$G_f(r, \theta, z; r_o, \theta_o, z_o; \omega) = -i \int_0^\infty \frac{k}{\nu} J_o(k[r^2 + r_o^2 - 2rr_o \cos(\theta - \theta_o)]^{1/2}) e^{-i\nu|z-z_o|} dk \quad (8)$$

or using Graf's addition theorem for Bessel functions:

$$G_f(r, \theta, z; r_o, \theta_o, z_o; \omega) = -i \int_0^\infty \frac{k}{\nu} \left[\sum_{m=0}^\infty \xi_m J_m(kr_o) J_m(kr) \cos(m[\theta - \theta_o]) \right] e^{-i\nu|z-z_o|} dk \quad (9)$$

with

$$\begin{aligned} \xi_m &= 2 \quad \text{for } m \neq 0 \\ \xi_m &= 1 \quad \text{for } m = 0 \end{aligned}$$

Equation (7) may then be written in the form:

$$\begin{aligned} \Phi_f(r, z, \omega) &= -i \int_0^\infty \frac{k}{\nu} \int_0^{2\pi} \left[\sum_{m=0}^\infty \xi_m J_m(kr_o) J_m(kr) \cos(m[\theta - \theta_o]) \right] \\ &\quad \times \int_{z_1}^{z_2} \tau(z_o, \theta_o) e^{-i\nu|z-z_o|} r_o d\theta_o dz_o dk \end{aligned} \quad (10)$$

where z_1 and z_2 denote the z -coordinates of the top and of the bottom of the borehole.

The assumptions that we have made about the source-borehole-formation geometry make the source density function τ independent of azimuth so that we get:

$$\Phi_f(r, z, \omega) = -i2\pi r_o \int_0^\infty \frac{k}{\nu} J_o(kr_o) J_o(kr) \int_{z_1}^{z_2} \tau(z_o) e^{-i\nu|z-z_o|} dz_o dk. \quad (11)$$

In order to evaluate the integral over z_o , we decompose the borehole wall into N cylindrical elements of height l . We choose l to be small enough so that τ may be assumed to be constant over one element. Equation (11) then becomes:

$$\Phi_f(r, z, \omega) = -i2\pi r_o \sum_{i=1}^N \tau_i \int_0^\infty \frac{k}{\nu} J_o(kr_o) J_o(kr) \left[\int_{-l/2}^{l/2} e^{-i\nu|z-(z_i+s)|} ds \right] dk. \quad (12)$$

The k -integral is calculated using the discrete wavenumber method, which gives:

$$\Phi_f(r, z, \omega) = \frac{-i4\pi^2 r_o}{L} \sum_{i=1}^N \tau_i \sum_{n=0}^M \frac{k_n}{\nu_n} J_o(k_n r_o) J_o(k_n r) \left[\int_{-l/2}^{l/2} e^{-i\nu_n|z-(z_i+s)|} ds \right]. \quad (13)$$

The integral over the element height s has a simple analytical expression which depends on the z -coordinate of the element relative to the observation point. Equation (13) can be used to calculate the expressions for the radial displacement u_r^f and radial stress σ_{rr}^f in the fluid. In order to evaluate the radial displacement at the borehole wall itself, however, one must add to the expression derived from equation (13) half of the radial displacement discontinuity which takes place across the particular source element on which the observation point is located (Sanchez-Sesma and Campillo, 1991; Coutant and Bouchon, 1992). This radial displacement discontinuity is easily evaluated mathematically and one gets:

$$u_r^f(r_o, z_j, \omega) = \frac{d\phi_f(r, z_j, \omega)}{dr} \Big|_{r=r_o} + 2\pi\tau_j. \quad (14)$$

The wavefield diffracted into the elastic formation may also be regarded, using Huygens principle, as arising from the radiation of secondary sources distributed all along the borehole wall. These forces are radial and vertical forces (Bouchon and Schmitt, 1989; Coutant, 1989). The displacement anywhere in the elastic formation may thus be written in the form:

$$u_j^e(r, z, \omega) = \int_{z_1}^{z_2} \int_0^{2\pi} \left[F_r(z_o, \theta_o) G_{jr}^e(r, \theta, z; r_o, \theta_o, z_o; \omega) + F_z(z_o, \theta_o) G_{jz}^e(r, \theta, z; r_o, \theta_o, z_o; \omega) \right] r_o d\theta_o dz_o \quad (15)$$

where F_r and F_z are the two force density functions, G^e is the Green tensor of the layered elastic formation and j denotes the r or z component.

The compressional and rotational displacement potentials radiated by a vertical point force of unit amplitude located at (r_o, θ_o, z_o) are (e.g., Müller, 1985):

$$\begin{aligned} \phi_z(r, \theta, z, \omega) &= \frac{1}{4\pi\rho\omega^2} \operatorname{sgn}(z - z_o) \int_0^\infty k J_o(k[r^2 + r_o^2 - 2rr_o \cos(\theta - \theta_o)]^{1/2}) e^{-i\nu|z - z_o|} dk \\ \psi_z(r, \theta, z, \omega) &= \frac{-i}{4\pi\rho\omega^2} \int_0^\infty \frac{k}{\gamma} J_o(k[r^2 + r_o^2 - 2rr_o \cos(\theta - \theta_o)]^{1/2}) e^{-i\nu|z - z_o|} dk \end{aligned} \quad (16)$$

with

$$\nu = \left(\frac{\omega^2}{\alpha^2} - k^2 \right)^{1/2}, \quad \operatorname{Im}(\nu) \leq 0; \quad \gamma = \left(\frac{\omega^2}{\beta^2} - k^2 \right)^{1/2}, \quad \operatorname{Im}(\gamma) \leq 0$$

and where α , β and ρ denote respectively the P- and S-wave velocities and density of the elastic medium surrounding the source.

Using Graf's addition theorem and integrating over θ_o one gets the displacement potentials radiated by a circular ring of vertical forces:

$$\begin{aligned} \phi_z^c(r, z, \omega) &= \frac{\operatorname{sgn}(z - z_o) r_o}{2\rho\omega^2} \int_0^\infty k J_o(kr_o) J_o(kr) e^{-i\nu|z - z_o|} dk \\ \psi_z^c(r, z, \omega) &= \frac{-i r_o}{2\rho\omega^2} \int_0^\infty \frac{k}{\gamma} J_o(kr_o) J_o(kr) e^{-i\gamma|z - z_o|} dk \end{aligned} \quad (17)$$

$$\begin{aligned} \text{where } \operatorname{sgn}(z - z_o) &= 1 & \text{if } z > z_o \\ \operatorname{sgn}(z - z_o) &= -1 & \text{if } z < z_o \end{aligned}$$

The P-SV displacement potentials produced by a unit radial force located at (r_o, θ_o, z_o) are:

$$\phi_r(r, \theta, z, \omega) = \frac{-i}{4\pi\rho\omega^2} \cos(\chi) \int_0^\infty \frac{k^2}{\nu} J_1(k[r^2 + r_o^2 - 2rr_o \cos(\theta - \theta_o)]^{1/2}) e^{-i\nu|z - z_o|} dk \quad (18)$$

$$\psi_r(r, \theta, z, \omega) = \frac{\text{sgn}(z - z_o)}{4\pi\rho\omega^2} \cos(\chi) \int_0^\infty J_1(k[r^2 + r_o^2 - 2rr_o \cos(\theta - \theta_o)]^{1/2}) e^{-i\gamma|z - z_o|} dk$$

where χ denotes the angle made at the source between the direction of the observation point and the radial direction.

The use of Graf's addition theorem and the integration over θ_o yields the displacement potentials radiated by a circular ring of radial forces:

$$\begin{aligned} \phi_r^c(r, z, \omega) &= \frac{ir_o}{2\rho\omega^2} \int_0^\infty \frac{k^2}{\nu} J_1(kr_o) J_o(kr) e^{-i\nu|z - z_o|} dk \\ \psi_r^c(r, z, \omega) &= \frac{-\text{sgn}(z - z_o)r_o}{2\rho\omega^2} \int_0^\infty J_1(kr_o) J_o(kr) e^{-i\gamma|z - z_o|} dk. \end{aligned} \quad (19)$$

The potentials radiated in the elastic formation by the i^{th} cylindrical vertical force element of the borehole wall are thus:

$$\begin{aligned} \Delta\Phi_z^i(r, z, \omega) &= \frac{F_{z,i}r_o}{2\rho\omega^2} \int_0^\infty k J_o(kr_o) J_o(kr) \left[\int_{-l/2}^{l/2} \text{sgn}[z - (z_i + s)] e^{-i\nu|z - (z_i + s)|} ds \right] dk \\ \Delta\Psi_z^i(r, z, \omega) &= \frac{-iF_{z,i}r_o}{2\rho\omega^2} \int_0^\infty \frac{k}{\gamma} J_o(kr_o) J_o(kr) \left[\int_{-l/2}^{l/2} e^{-i\gamma|z - (z_i + s)|} ds \right] dk. \end{aligned} \quad (20)$$

Similarly the potentials radiated by the i^{th} cylindrical radial force element are:

$$\begin{aligned} \Delta\Phi_r^i(r, z, \omega) &= \frac{iF_{r,i}r_o}{2\rho\omega^2} \int_0^\infty \frac{k^2}{\nu} J_1(kr_o) J_o(kr) \left[\int_{-l/2}^{l/2} e^{-i\nu|z - (z_i + s)|} ds \right] dk \\ \Delta\Psi_r^i(r, z, \omega) &= \frac{-F_{r,i}r_o}{2\rho\omega^2} \int_0^\infty J_1(kr_o) J_o(kr) \left[\int_{-l/2}^{l/2} \text{sgn}[z - (z_i + s)] e^{-i\gamma|z - (z_i + s)|} ds \right] dk. \end{aligned} \quad (21)$$

As before the k -integrals are calculated using the discrete wavenumber method, which gives:

$$\begin{aligned} \Delta\Phi_z^i(r, z, \omega) &= \frac{F_{z,i}\pi r_o}{L\rho\omega^2} \sum_{n=0}^M k_n J_o(k_n r_o) J_o(k_n r) \left[\int_{-l/2}^{l/2} \text{sgn}[z - (z_i + s)] e^{-i\nu_n|z - (z_i + s)|} ds \right] \\ \Delta\Psi_z^i(r, z, \omega) &= \frac{-iF_{z,i}\pi r_o}{L\rho\omega^2} \sum_{n=0}^M \frac{k_n}{\gamma_n} J_o(k_n r_o) J_o(k_n r) \left[\int_{-l/2}^{l/2} e^{-i\gamma_n|z - (z_i + s)|} ds \right]. \end{aligned} \quad (22)$$

Similarly the potentials radiated by the i^{th} cylindrical radial force element are:

$$\Delta\Phi_r^i(r, z, \omega) = \frac{iF_{r,i}\pi r_o}{L\rho\omega^2} \sum_{n=0}^M \frac{k_n^2}{\nu_n} J_1(k_n r_o) J_o(k_n r) \left[\int_{-l/2}^{l/2} e^{-i\nu_n|z - (z_i + s)|} ds \right] \quad (23)$$

$$\Delta \Psi_r^i(r, z, \omega) = \frac{-F_{r,i} \pi r_o}{L \rho \omega^2} \sum_{n=0}^M J_1(k_n r_o) J_0(k_n r) \left[\int_{-l/2}^{l/2} \operatorname{sgn}[z - (z_i + s)] e^{-i\gamma_n |z - (z_i + s)|} ds \right]$$

with $\nu_n = \left(\frac{\omega^2}{\alpha^2} - k_n^2 \right)^{1/2}$, $\operatorname{Im}(\nu_n) \leq 0$
 $\gamma_n = \left(\frac{\omega^2}{\beta^2} - k_n^2 \right)^{1/2}$, $\operatorname{Im}(\gamma_n) \leq 0$.

These source potentials can be combined with the reflectivity and transmissivity matrices of the layered elastic formation (Kennett, 1974; Müller, 1985) to calculate the wavefield anywhere in the formation. When calculating the stresses on the element itself, however, one must add to the expressions derived from equations (22–23) half of the stress discontinuities across the source element considered (Sanchez-Sesma and Campillo, 1991; Coutant and Bouchon, 1992), that is:

$$\frac{\delta \sigma_{rr}}{2} = -\frac{F_{r,i}}{2}$$

$$\frac{\delta \sigma_{rz}}{2} = -\frac{F_{z,i}}{2}$$

One can then calculate the radial displacement and the normal and tangential stresses at the borehole wall as a function of the radial and vertical force density functions. The matching of the boundary conditions at the middle of each borehole element between the displacement-stress field calculated in the fluid and the one calculated in the formation then leads to the system of equations:

$$\begin{aligned} u_{r,i}^c &= u_{r,i}^f + u_{r,i}^s \\ \sigma_{rr,i}^e &= \sigma_{rr,i}^f + \sigma_{rr,i}^s \\ \sigma_{rz,i}^e &= 0 \end{aligned} \quad (24)$$

with $i = 1, N$

from which the source density distributions τ_i , $F_{z,i}$, $F_{r,i}$ can be obtained by inversion.

EXAMPLES OF APPLICATION

The first application that we consider is the simulation of a full wave acoustic log. The elastic formation is homogeneous except for the presence of a 1m thick low velocity layer. The P- and S-wave velocities and density are respectively 3000m/s, 1700m/s and 2.7 outside the layer, and 2000m/s, 850m/s and 2.4 inside the layer. The borehole has a radius of 12cm and is filled with a fluid of density equal to 1.0 and compressional wave velocity of 1500m/s. The source is located 2m above the layer interface and its time function is a pulse of dilatation whose mathematical expression is chosen as a twice-integrated Ricker wavelet of 2.5kHz central frequency. The receiver array consists of 41

pressure sensors located at the center of the borehole between distances of 1m and 5m from the source. The calculation is made over a time window of length $T_l = 4ms$ and for 64 frequencies. The imaginary part of the frequency used in the discrete wavenumber calculation is $\omega_i = -\pi/T_l$.

The length of borehole considered is 9m and the source is located 4m below the upper extremity of the borehole. The number of elements used to represent the borehole varies with frequency. At low frequencies a minimum number of 180 elements is assumed while at high frequencies the number of elements is chosen such that the element height l is equal to about one third of the shortest wavelength. For the borehole portion located within the layer, the shortest wavelength is associated with the formation shear wave, while it is the fluid compressional wave wavelength elsewhere. The element height is thus different in each layer.

The results of this calculation are displayed in Figure 1. For the frequency range considered, the Stoneley wave dominates the acoustic log. Its waveform is strongly affected by the crossing of the low-velocity layer. At depths below the layer, the main Stoneley pulse is preceded by another tube wave arrival which is produced by a conversion from P wave to Stoneley wave at the bottom of the layer. The upgoing tube waves reflected at the layer interfaces have about 15% of the amplitude of the downgoing Stoneley wave.

The second application that we consider involves the calculation of the wavefield inside the formation. The geological formation still consists of a low-velocity layer (P-wave velocity = 2000m/s, S-wave velocity = 850m/s, density = 2.4) sandwiched between two homogeneous half-spaces of identical elastic parameters (P-wave velocity = 3000m/s, S-wave velocity = 1700m/s, density = 2.7). The layer thickness is 4m and the borehole is filled with water (P-wave velocity = 1500m/s, density = 1.0) and has a radius of 15 cm. The source is located 5m above the layer and is a pulse of dilatation whose mathematical expression is a twice-integrated Ricker wavelet of central frequency equal to 1kHz. The radial displacement generated by the source is calculated along a vertical profile located 30m away from the borehole. The receiver array extends over 60m and is centered on the source depth. The borehole length considered is 90m (from 45m above the source to 45m below) and the radial periodicity interval L is 180m. The length of the time window is 0.06s and the calculation is made over 112 frequencies. The number of elements considered varies between 190 (at low frequencies) and 350 (at the highest frequency) with the same element-height versus shortest wavelength criterion as in the previous simulation.

The results obtained are displayed in Figure 2. Numerous wavefronts are identifiable. The energy conversion which takes place where the borehole intersects the low-velocity layer results in a considerable feeding of seismic energy into the layer. The guided wave pattern of the wavefield inside the layer is clearly apparent in Figure 3 where only the receivers located in the layer and close to it are considered. The wavefield in the layer is made up of downgoing and upgoing wave packets reflected at the layer boundaries.

At each bounce of these wave packets a small amount of energy is radiated into the rest of the formation.

Because of the radial periodicity chosen (180m) and the formation fastest wave velocity (3000m/s), one may expect at the receivers located above the layer a parasitic P wave arrival at about 0.05s which originates from the first source image (Bouchon, 1981). This arrival associated with a very small moveout can be indeed identified on the section.

Parasitic arrivals may also be generated by the imposed finiteness of the borehole. When the wavefield emitted by the source, particularly the tube wave, reaches the extremities of the borehole, some diffraction occurs and may cause unwanted arrivals. Such disturbances are easily identifiable because they display negative moveouts. One such disturbance can be discerned on Figure 2. It arrives at about 0.05s on the upper trace and at increasingly later times on the traces below before disappearing. Its travel-time corresponds to a conversion from Stoneley wave to shear wave at the upper extremity of the borehole.

CONCLUSION

We have presented a semi-analytical, semi-numerical method to calculate the diffraction of acoustic and elastic waves at the boundary between a fluid-filled cylindrical borehole and a layered elastic medium. The method is formulated as a boundary element technique where the Green's functions are evaluated by the discrete wavenumber method. We have shown that the method is well suited to compute synthetic acoustic logs when the geological formation surrounding the borehole is layered and to study the seismic wavefield radiated into the formation as well as its subsequent propagation.

REFERENCES

- Bouchon, M., 1981, A simple method to calculate Green's functions for elastic layered media: *Bull. Seism. Soc. Am.*, 71, 959-971.
- Bouchon, M., 1985, A simple, complete numerical solution to the problem of diffraction of SH waves by an irregular interface: *J. Acoust. Soc. Am.*, 77, 1-5.
- Bouchon, M., Campillo, M., and Gaffet, S., 1989, A boundary integral equation discrete wavenumber representation method to study wave propagation in multilayered media having irregular interfaces: *Geophysics*, 54, 1134-1140.
- Bouchon, M., and Schmitt, D.P., 1989, Full-wave acoustic logging in an irregular bore-

- hole: *Geophysics*, 54, 758–765.
- Campillo, M., 1987a, Lg wave propagation in a laterally varying crust and the distribution of the apparent quality factor in central France: *J. Geophys. Res.*, 92, 12604–12614.
- Campillo, M., 1987b, Modeling of SH-wave propagation in an irregularly layered medium—Application to seismic profiles near a dome: *Geophys. Prosp.*, 35, 236–249.
- Cheng, C.H., and Toksöz, M.N., 1981, Elastic wave propagation in a fluid-filled borehole and synthetic acoustic logs: *Geophysics*, 46, 1042–1053.
- Cheng, C.H., Toksöz, M.N., and Willis, M.E., 1982, Determination of in situ attenuation from full waveform acoustic logs: *J. Geophys. Res.*, 87, 5477–5484.
- Coutant, O., 1989, Numerical study of the diffraction of elastic waves by fluid-filled cracks: *J. Geophys. Res.*, 94, 17805–17818.
- Coutant, O., and Bouchon, M., 1992, Boundary integral equation discrete wavenumber decomposition method for elastic wave propagation simulation: correction and approximation: in preparation.
- Gaffet, S., and Bouchon, M., 1991, Source location and valley shape effects on the P-SV displacement field using a boundary integral equation-discrete wavenumber representation method: *Geophys. J. Int.*, 106, 341–355.
- Kawase, H., 1988, Time-domain response of a semicircular canyon for incident SV, P, and Rayleigh waves calculated by the discrete wavenumber boundary element method: *Bull. Seism. Soc. Am.*, 78, 1415–1437.
- Kawase, H., and Aki, K., 1989, A study of the response of a soft basin for incident S, P, and Rayleigh waves with special reference to the long duration observed in Mexico City: *Bull. Seism. Soc. Am.*, 79, 1361–1382.
- Kawase, H., and Aki, K., 1990, Topography effect at the critical SV incidence: possible explanation of damage pattern by the Whittier Narrows, California, earthquake of 1 October 1987: *Bull. Seism. Soc. Am.*, 80, 1–22.
- Kennett, B.L.N., 1974, Reflections, rays and reverberations: *Bull. Seism. Soc. Am.*, 65, 1643–1651.
- Kurkjian, A.L., and Chang, S.K., 1986, Acoustic multipole sources in fluid-filled boreholes: *Geophysics*, 51, 148–163.
- Liu, H.L., and Randall, C.J., 1991, Synthetic waveforms in noncircular boreholes using a boundary integral equation method: *61st SEG Ann. Mtg. Expanded Abstracts*,

843-845.

- Müller, G., 1985, The reflectivity method: a tutorial: *J. Geophys.*, *58*, 153-174.
- Paul, A., and Campillo, M., 1988, Diffraction and conversion of elastic waves at a corrugated interface: *Geophysics*, *53*, 1415-1424.
- Randall, C.J., 1991, Modes of noncircular fluid-filled boreholes in elastic formations: *J. Acoust. Soc. Am.*, *89*, 1002-1016.
- Randall, C.J., Scheibner, D.J., and Wu, P.T., 1991, Multipole borehole acoustic waveforms: synthetic logs with beds and borehole washouts: *Geophysics*, *56*, 1757-1769.
- Sanchez-Sesma, F.J., and Campillo, M., 1991, Diffraction of P, SV, and Rayleigh waves by topographic features: a boundary integral formulation: *Bull. Seism. Soc. Am.*, *81*, 2234-2253.
- Sanchez-Sesma, F.J., and Esquivel, J., 1979, Ground motion on alluvial valleys under incident plane SH waves: *Bull. Seism. Soc. Am.*, *69*, 1107-1120.
- Schmitt, D.P., 1988, Shear wave logging in elastic formations: *J. Acoust. Soc. Am.*, *84*, 2215-2229.
- Schmitt, D.P., and Bouchon, M., 1985, Full-wave acoustic logging: synthetic microseismograms and frequency-wavenumber analysis: *Geophysics*, *50*, 1756-1778.
- Schoenberg, M., Marzetta, T., Aron, J., and Porter, R.P., 1981, Space-time dependence of acoustic waves in a borehole: *J. Acoust. Soc. Am.*, *70*, 1496-1507.
- Stephen, R.A., Pardo-Casas, F., and Cheng, C.H., 1985, Finite-difference synthetic acoustic logs: *Geophysics*, *50*, 1588-1609.
- Tsang, L., and Rader, D., 1979, Numerical evaluation of the transient elastic waveform due to a point source in a fluid-filled borehole: *Geophysics*, *44*, 1706-1720.
- Tubman, K.M., Cheng, C.H., and Toksöz, M.N., 1984, Synthetic full-waveform acoustic logs in cased boreholes: *Geophysics*, *49*, 1051-1059.

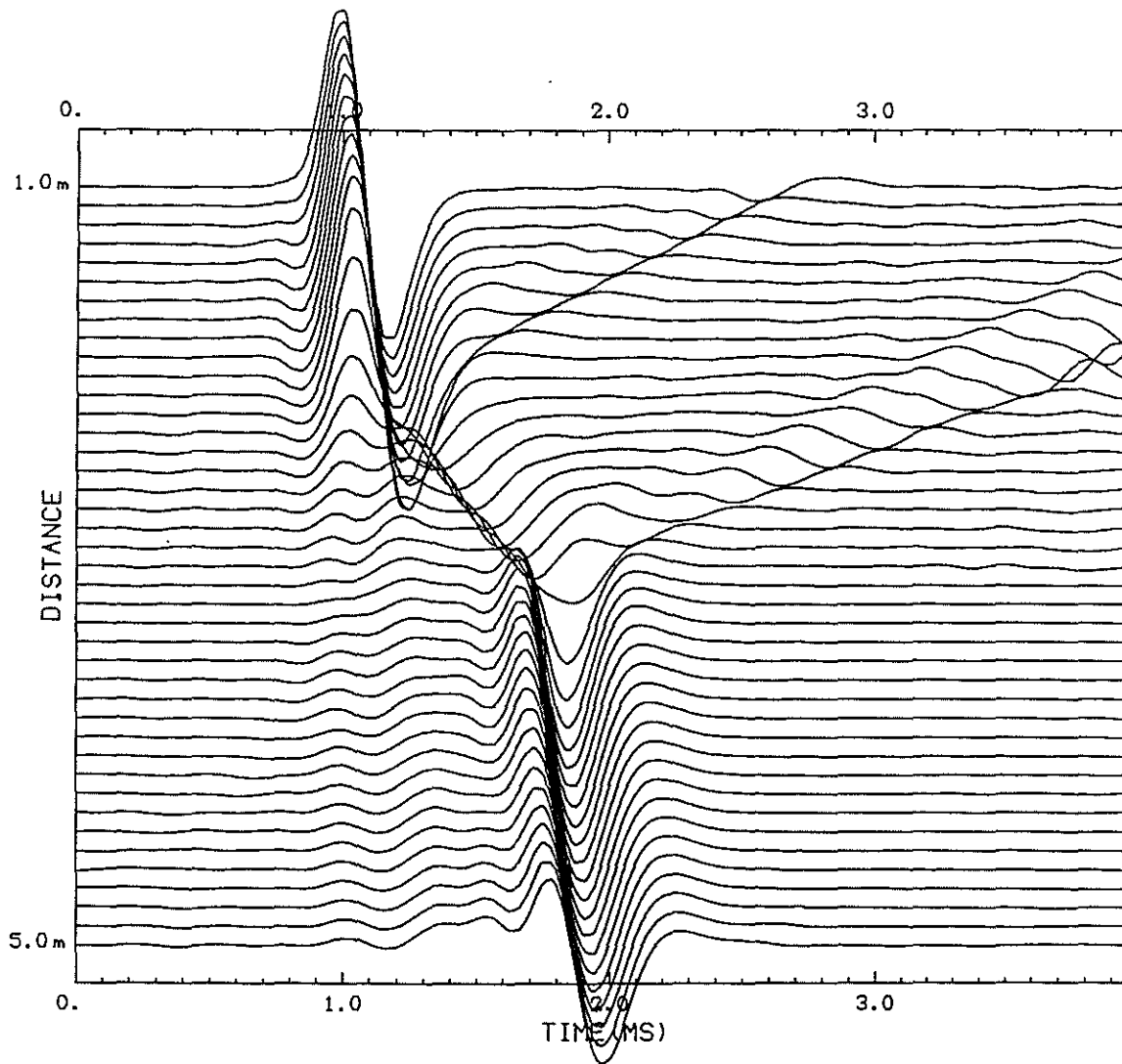


Figure 1: Synthetic acoustic log calculated for the geometry and elastic parameters given in the text. Distances are measured from the source. A reduction velocity equal to the fluid P-wave velocity (1500m/s) has been applied to the traces.

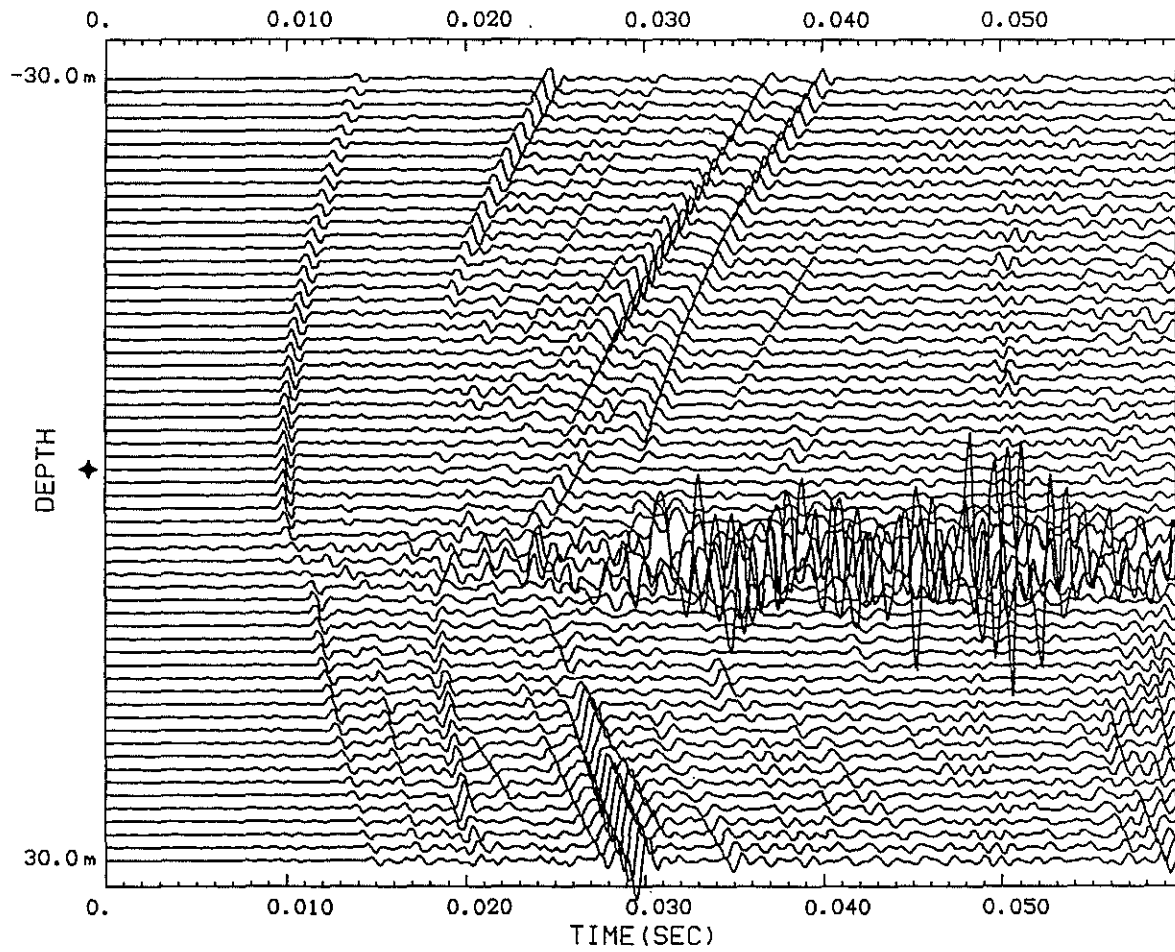


Figure 2: Traces of the radial displacement along a vertical profile at a distance of 30m from the source borehole. The geometry and elastic parameters are given in the text. The depth indicated is relative to the source depth which is identified by a star.

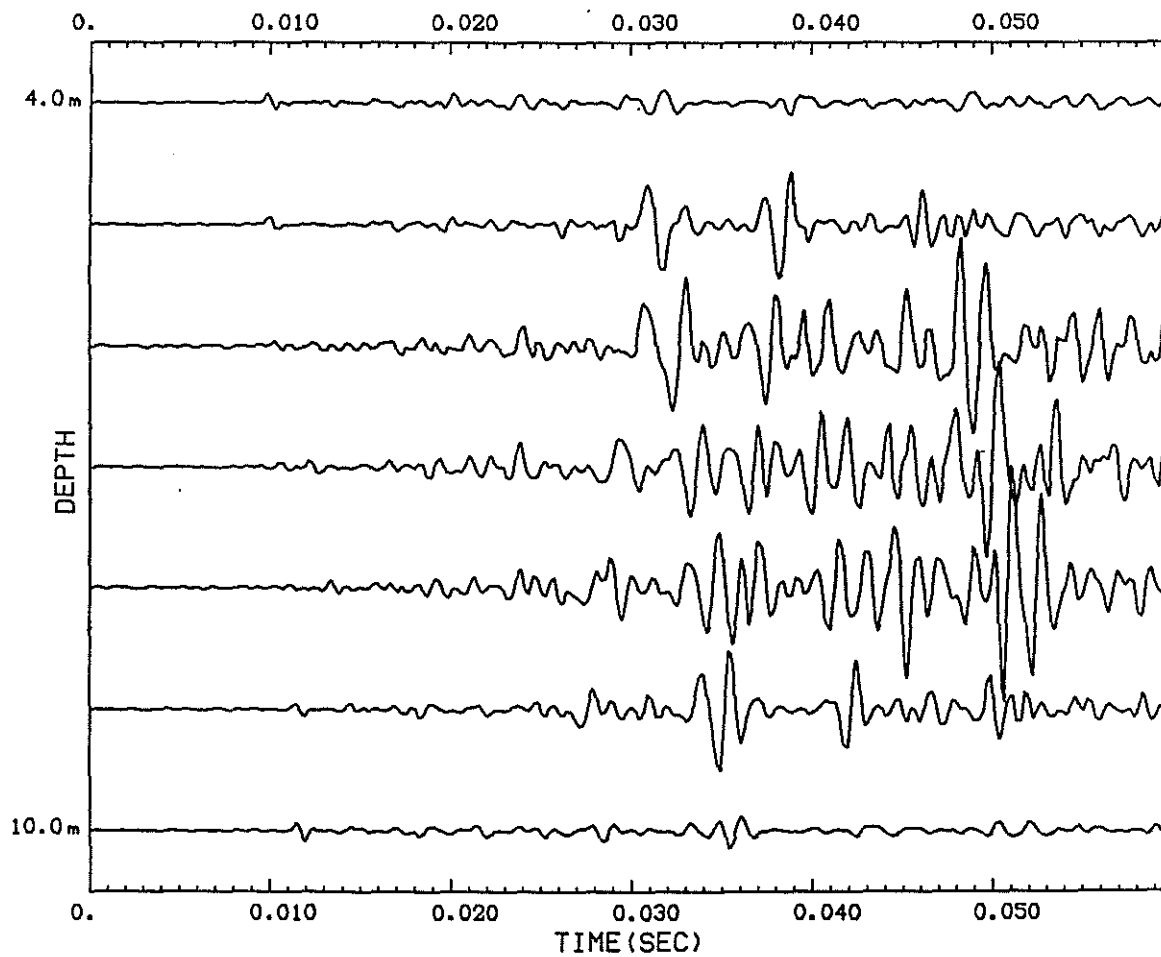


Figure 3: Enlarged picture of the area of Figure 2 corresponding to receivers inside or near the low-velocity layer.